

## Central Lancashire Online Knowledge (CLOK)

|          |  |
|----------|--|
| Title    | In situ XPS of Competitive CO <sub>2</sub> /H <sub>2</sub> O Absorption in an Ionic Liquid   |
| Type     | Article  |
| URL      | <a href="https://clock.uclan.ac.uk/49146/">https://clock.uclan.ac.uk/49146/</a>  |
| DOI      | ##doi##  |
| Date     | 2023   |
| Citation | Cole, Jordan, Henderson, Zoe, Thomas, Andrew G, Castle, Christopher, Greer, Adam, Hardacre, Christopher, Scardamaglia, Mattia, Shavorskiy, Andrey and Syres, Karen orcid iconORCID: 0000-0001-7439-475X (2023) In situ XPS of Competitive CO <sub>2</sub> /H <sub>2</sub> O Absorption in an Ionic Liquid. Journal of Physics: Materials . |
| Creators | Cole, Jordan, Henderson, Zoe, Thomas, Andrew G, Castle, Christopher, Greer, Adam, Hardacre, Christopher, Scardamaglia, Mattia, Shavorskiy, Andrey and Syres, Karen   |

It is advisable to refer to the publisher's version if you intend to cite from the work. ##doi##

For information about Research at UCLan please go to <http://www.uclan.ac.uk/research/>

All outputs in CLOK are protected by Intellectual Property Rights law, including Copyright law. Copyright, IPR and Moral Rights for the works on this site are retained by the individual authors and/or other copyright owners. Terms and conditions for use of this material are defined in the <http://clock.uclan.ac.uk/policies/>

ACCEPTED MANUSCRIPT • OPEN ACCESS

## In situ XPS of Competitive CO<sub>2</sub>/H<sub>2</sub>O Absorption in an Ionic Liquid

To cite this article before publication: Jordan Cole *et al* 2023 *J. Phys. Mater.* in press <https://doi.org/10.1088/2515-7639/acfdcf>

### Manuscript version: Accepted Manuscript

Accepted Manuscript is “the version of the article accepted for publication including all changes made as a result of the peer review process, and which may also include the addition to the article by IOP Publishing of a header, an article ID, a cover sheet and/or an ‘Accepted Manuscript’ watermark, but excluding any other editing, typesetting or other changes made by IOP Publishing and/or its licensors”

This Accepted Manuscript is © 2023 The Author(s). Published by IOP Publishing Ltd.



As the Version of Record of this article is going to be / has been published on a gold open access basis under a CC BY 4.0 licence, this Accepted Manuscript is available for reuse under a CC BY 4.0 licence immediately.

Everyone is permitted to use all or part of the original content in this article, provided that they adhere to all the terms of the licence <https://creativecommons.org/licenses/by/4.0>

Although reasonable endeavours have been taken to obtain all necessary permissions from third parties to include their copyrighted content within this article, their full citation and copyright line may not be present in this Accepted Manuscript version. Before using any content from this article, please refer to the Version of Record on IOPscience once published for full citation and copyright details, as permissions may be required. All third party content is fully copyright protected and is not published on a gold open access basis under a CC BY licence, unless that is specifically stated in the figure caption in the Version of Record.

View the [article online](#) for updates and enhancements.

# *In situ* XPS of Competitive CO<sub>2</sub>/H<sub>2</sub>O Absorption in an Ionic Liquid

Jordan Cole<sup>1</sup>, Zoë Henderson<sup>1</sup>, Andrew G. Thomas<sup>2</sup>, Christopher Castle<sup>3</sup>, Adam J. Greer<sup>4</sup>, Christopher Hardacre<sup>4</sup>, Mattia Scardamaglia<sup>5</sup>, Andrey Shavorskiy<sup>5</sup>, and Karen L. Syres<sup>1</sup>

<sup>1</sup> Jeremiah Horrocks Institute for Mathematics, Physics and Astronomy, University of Central Lancashire, Preston, PR1 2HE, UK

<sup>2</sup> Department of Materials Science, Photon Science Institute and Henry Royce Institute, University of Manchester, Manchester, M13 9PL, UK

<sup>3</sup> Department of Physics and Astronomy, and Photon Science Institute, University of Manchester, Manchester, M13 9PL, UK

<sup>4</sup> Department of Chemical Engineering and Analytical Science, University of Manchester, Manchester, M13 9PL, UK

<sup>5</sup> MAX IV Laboratory, University of Lund, 22100, Lund, Sweden

\*Email: KSyres@uclan.ac.uk; JCole4@uclan.ac.uk

## Email:

KSyres@uclan.ac.uk; JCole4@uclan.ac.uk

Received xxxxxx

Accepted for publication xxxxxx

Published xxxxxx

## Abstract

Superbasic ionic liquids (SBILs) are being investigated as potential CO<sub>2</sub> gas capture agents, however, the presence of H<sub>2</sub>O in the flue stream can inhibit the uptake of CO<sub>2</sub>. In this study a thin film of the SBIL trihexyltetradecylphosphonium 1,2,4-triazolide ([P<sub>66614</sub>][124Triz]) was deposited onto rutile TiO<sub>2</sub> (110) using *in situ* electrospray deposition and studied upon exposure to CO<sub>2</sub> and H<sub>2</sub>O using *in situ* near-ambient pressure X-ray photoelectron spectroscopy (NAP-XPS). The molar uptake ratio of gas in the electrosprayed SBIL ( $n_{gas}:n_{IL}$ ) was calculated to be 0.3:1 for CO<sub>2</sub>, 0.7:1 for H<sub>2</sub>O, and 0.9:1 for a CO<sub>2</sub>/H<sub>2</sub>O mixture. NAP-XPS taken at two different depths reveals that the competitive absorption of CO<sub>2</sub> and H<sub>2</sub>O in [P<sub>66614</sub>][124Triz] varies with sampling depth. A greater concentration of CO<sub>2</sub> adsorbs in the bulk layers, while more H<sub>2</sub>O adsorbs at the surface. The presence of H<sub>2</sub>O in the gas mixture does not inhibit the absorption of CO<sub>2</sub>. Measurements taken during exposure and after the removal of gas indicate that CO<sub>2</sub> adsorbed in the bulk does so reversibly, whilst CO<sub>2</sub> adsorbed at the surface does so irreversibly. This is contrary to the fully reversible CO<sub>2</sub> reaction shown for bulk ILs in literature and suggests that irreversible absorption of CO<sub>2</sub> in our highly-structured thin films is largely attributed to reactions at the surface. This has potential implications on IL gas capture and thin film IL catalysis applications.

Keywords: ionic liquids, carbon capture, x-ray photoelectron spectroscopy, thin films, electrospray

## 1. Introduction

The capture and sequestration of carbon dioxide (CO<sub>2</sub>) has been an important process in the reduction of CO<sub>2</sub> emissions in recent years. Currently, fossil fuel-fired power plants use

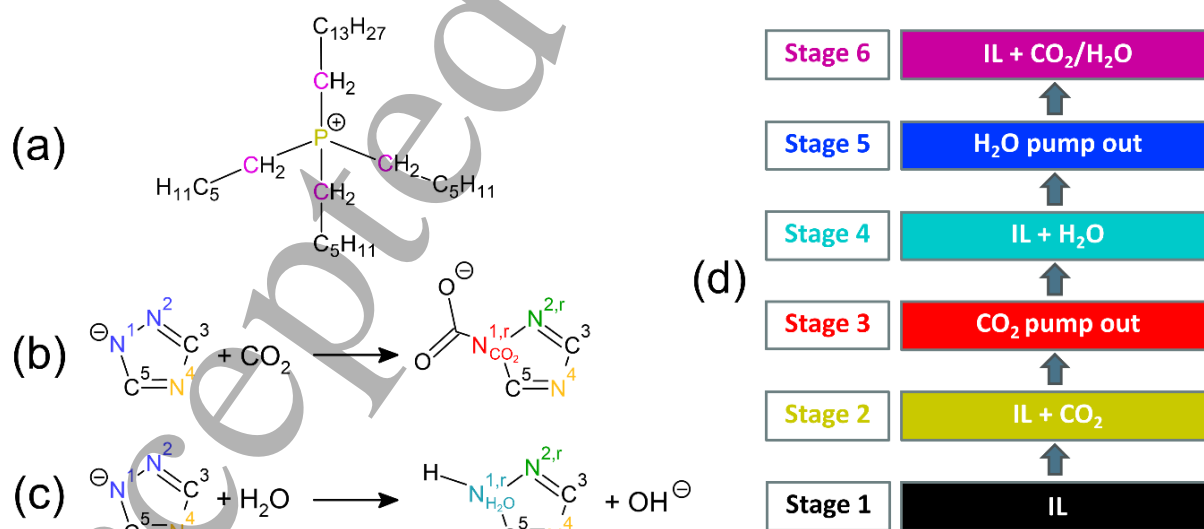
alkanolamine solvents such as monoethanolamine (MEA) for CO<sub>2</sub> capture. Despite reducing a power plant's CO<sub>2</sub> emissions by as much as 90% [1], these industrial solvents generate problems of their own, with issues such as toxicity and long-term costs challenging their suitability [2]. Ionic liquids (ILs) have seen a recent growth of interest as promising green and non-toxic alternatives to current CO<sub>2</sub> capture solvents. ILs are liquid salts consisting of pairs of bulky anions and cations held together by strong Coulombic forces [3]. The chemical and physical properties of an IL can be fine-tuned via the cation-anion pair. Their high CO<sub>2</sub> capacity, very low volatility, high thermal stability, and lower regeneration temperature compared to MEA make them desirable alternatives [4–6]. The tunability, low melting points and wide electrochemical windows of ILs have led to their use in a wide range of other applications across electrochemistry (electrolytes for batteries [7], nanostructure growth [8,9], and solar cells [10,11]), tribology (lubricants [12,13] and corrosion inhibitors [14]) and catalysis (SCILL and SILP catalysts [15,16]).

An important property for ILs in carbon capture is their selectivity for CO<sub>2</sub>. Industrial flue gas contains a complex mixture of gases such as CO<sub>2</sub>, H<sub>2</sub>O, O<sub>2</sub>, N<sub>2</sub>, CO, SO<sub>x</sub> and NO<sub>x</sub> [17,18]. Therefore, it is vital to understand the effect of a mixture of gases on the IL and how they compete for absorption. For conventional ILs with imidazolium-based cations, the anion has been found to be responsible for the solubility of these gases [19,20], but also dictates some of the physical properties of the IL such as its density, viscosity and melting point [21]. Alternatives to conventional physically absorbing ILs came in the way of anion-functionalised task-specific ILs which chemically absorb CO<sub>2</sub>, leading to higher CO<sub>2</sub> capacities [6,22]. These ILs, however, suffer increased viscosity upon absorption of CO<sub>2</sub>, which consequently hinders further CO<sub>2</sub> absorption and limits their current applicability

[23,24]. An emerging class of ILs called superbasic ILs (SBILs) show great promise for CO<sub>2</sub> capture due to their higher CO<sub>2</sub> capacity compared to conventional ILs and the ability to chemically and reversibly absorb CO<sub>2</sub> without significant changes in their viscosity [25].

Commonly, SBILs have phosphonium-based cations and imidazolium-based anions, with anions such as [benzim]<sup>−</sup> and [124Triz]<sup>−</sup> yielding the highest CO<sub>2</sub> capacities and solubilities [26,27]. In SBILs, the anion chemically reacts with CO<sub>2</sub> in the same way as MEA, forming a carbamate species [22]. In fact, the SBIL [P<sub>66614</sub>][124Triz] is able to both chemically and physically absorb CO<sub>2</sub> [28]. Mercy *et al.* used DFT simulations to study CO<sub>2</sub> capture in the SBIL [P<sub>3333</sub>][124Triz] [29]. They found that while the cation plays no direct role in the chemisorption of CO<sub>2</sub>, the presence of the cation increases the negative charge of the N<sup>1</sup> nitrogen site in [124Triz]<sup>−</sup> (see Scheme 1(b)). This increases the reactivity on N<sup>1</sup>, which is considered the most favourable reaction site in the anion. Unlike conventional physically absorbing ILs, SBILs are capable of achieving greater than equimolar amounts of CO<sub>2</sub> absorption. Taylor *et al.* reported a CO<sub>2</sub> uptake of 1.20:1 (*n*<sub>CO<sub>2</sub></sub>:*n*<sub>IL</sub>) in the dry state for the SBIL trihexyltetradecylphosphonium benzimidazole, [P<sub>66614</sub>][benzim] [26]. SBILs have been found to only experience minor reductions in CO<sub>2</sub> capacity in the presence of water [26], SO<sub>2</sub> [30], and NO [25], and in some cases preferentially and reversibly absorb CO<sub>2</sub> in the presence of other gases [31].

X-ray photoelectron spectroscopy (XPS) is a technique traditionally carried out at ultra-high vacuum, but advancements in electron optics and the use of synchrotron light and instrumentation have driven development of the technique to near-ambient pressures (up to about 20 mbar) which allows investigations of liquid/gas interfaces [32]. This



**Scheme 1.** (a) Chemical structure of the [P<sub>66614</sub>]<sup>+</sup> cation with C<sub>hetero</sub> atoms highlighted in magenta and C<sub>aliphatic</sub> in black. The reaction scheme for [124Triz]<sup>−</sup> with (b) CO<sub>2</sub> and (c) H<sub>2</sub>O. Atoms N<sup>1</sup> and N<sup>2</sup> (blue) are equivalent due to resonance effects. Reaction with CO<sub>2</sub> at N<sup>1</sup> results in the formation of carbamate. Reaction with H<sub>2</sub>O forms triazole and a hydroxide ion. N<sup>1,r</sup> (red, light blue) and N<sup>2,r</sup> (green) denote the N atoms following reaction of the anion with CO<sub>2</sub> or H<sub>2</sub>O. (d) Gas exposure regime for the ESD1 [P<sub>66614</sub>][124Triz] electrospayed thin film.

technique has been used to study interactions between ILs and gases [31,33–35], including SBILs [31]. For example, a study by Henderson *et al.* revealed that the adsorption of water vapour at the surface of ultra-thin films of [C<sub>4</sub>C<sub>1</sub>Im][BF<sub>4</sub>] induced a reordering of the ions at the IL/gas interface [34]. Water vapour remained trapped at the surface for some time even after the gas was evacuated. Greer *et al.* investigated the competitive absorption of CO<sub>2</sub> and NO in [P<sub>66614</sub>][benzim] [25]. Although the absorption of NO resulted in irreversible bonding of NONOate species to the [benzim]<sup>-</sup> anion, the presence of NO had little effect on the reversibility of CO<sub>2</sub> absorption and the CO<sub>2</sub> capacity of the IL.

There is currently limited information on how interactions between CO<sub>2</sub> molecules and the IL influence structure and ordering at the IL/gas interface, and how these interactions vary through the IL layers. Herein, we report an *in situ* near-ambient pressure XPS study into the ordering and interactions of electro sprayed thin films of the SBIL [P<sub>66614</sub>][124Triz] on rutile TiO<sub>2</sub> (110) before, during, and after exposure to CO<sub>2</sub> and H<sub>2</sub>O. To the best of our knowledge, this will be the first use of NAP-XPS at two different sampling depths to study CO<sub>2</sub> absorption in ILs. These results provide new insights into competitive absorption of CO<sub>2</sub> and H<sub>2</sub>O in SBILs and the reversibility of these reactions. Results indicate that more CO<sub>2</sub> absorbs in the bulk layers of the thin film, and this absorption is reversible. However, less CO<sub>2</sub> ad/absorbs at the surface and the ad/absorption is irreversible. Water vapour reversibly ad/absorbs at the surface and does so in greater concentrations compared to the bulk layers.

## 2. Method

Experimental measurements of the SBIL trihexyltetradecylphosphonium 1,2,4-triazolide ([P<sub>66614</sub>][124Triz], structure shown in Scheme 1) were carried out at beamline HIPPIE at MAX-IV synchrotron in Sweden (photon energy range 255 – 2200 eV) [36]. The HIPPIE endstation analysis chamber has a hemispherical Scienta-Omicron HiPP-3 electron energy analyser positioned in the plane of the storage ring at 55° to the direction of the incoming X-ray beam [36]. A near-ambient pressure cell is docked to the analyser to carry out near-ambient pressure experiments. All XPS measurements were taken at normal emission (giving a 35° angle between the incident X-ray beam and the sample surface).

A rutile TiO<sub>2</sub> (110) single crystal (PI-KEM) was cleaned via Ar<sup>+</sup> sputter/anneal cycles (sputtering at 1 keV for 10 minutes and annealing at 700°C for 10 minutes) until XPS spectra showed no contamination. [P<sub>66614</sub>][124Triz] was deposited onto the rutile TiO<sub>2</sub> (110) substrate via electro spray deposition in vacuum using a Molecular spray UHV4 system. The deposition chamber had a base pressure of 2.0 × 10<sup>-10</sup> mbar and a deposition pressure of 7.0 × 10<sup>-10</sup> mbar. A 0.02 M [P<sub>66614</sub>][124Triz]/methanol solution was fed into the emitter

capillary by a syringe pump delivering a flow rate of 0.3 ml/h. The emitter, syringe and tubing were cleaned prior to use by flushing with the solvent. 3.0 kV was applied to the emitter with respect to the grounded entrance capillary. Two electro spray thin films were deposited, a 2.3 ± 0.6 nm (electro spray deposition 1, ESD1) and a 6.2 ± 1.8 nm (ESD2) thin film. Film thickness calculations are given in the Supplementary Information (SI). A beam damage study showed no degradation of the IL upon prolonged exposure to the beam, but the sample was still moved ~ 0.1 mm between scans to avoid possible charging and degradation of the IL.

The ESD1 thin film of [P<sub>66614</sub>][124Triz] was characterised using photoemission while exposed to CO<sub>2</sub>, H<sub>2</sub>O and finally a CO<sub>2</sub>/H<sub>2</sub>O gas mixture. The IL film was exposed to each of the gases for about 2 hours whilst XPS scans were taken. Gases were leaked into the NAP cell at approximately 1 mbar at room temperature. The molar ratio of CO<sub>2</sub>:H<sub>2</sub>O in the gas mixture was 1.1:1 ± 0.1, calculated using the areas of the gas-phase peaks in the O 1s spectra. Measurements were taken during exposure and after the gas was pumped out of the NAP cell after each stage in order to study the reversibility of absorption. This exposure procedure is detailed in Scheme 1(d). An XPS study was carried out at two different depths on the [P<sub>66614</sub>][124Triz] ESD2 thin film by changing the photon energy as summarised in Table 1. These photon energies result in photoelectrons with maximum kinetic energies of 150 and 600 eV, corresponding to surface and bulk sampling depths, respectively. Surface and bulk layers of the ESD2 6.2 nm thin film were probed at sampling depths of 1.6 and 4.0 nm, respectively. Measurements were taken before exposure, during exposure to CO<sub>2</sub>, and during exposure to H<sub>2</sub>O, both at 1 mbar (2 hour gas exposure time). A summary of the photon energies used for each photoemission region is presented in Table 1.

All XPS peaks have been fitted using 30:70 (Lorentzian:Gaussian) line shapes and a linear background, using the software CasaXPS [37]. The binding energy (BE) scale for all regions has been calibrated to the alkyl C 1s signal at 285.0 eV and all fitted peaks are quoted to ± 0.1 eV BE [38].

## 3. Results

### 3.1 [P<sub>66614</sub>][124Triz] NAP-XPS

NAP-XPS measurements were carried out on an electro sprayed 2.3 nm thin film (ESD1) of the IL [P<sub>66614</sub>][124Triz]. These were taken as the IL was exposed to CO<sub>2</sub>, H<sub>2</sub>O, and finally a CO<sub>2</sub>/H<sub>2</sub>O mixture, all at 1 mbar. Measurements were also taken prior to exposure and after the gas was removed between each exposure stage, as summarised in Scheme 1(d), in order to investigate the reversibility of absorption. Survey spectra taken at each stage of exposure are shown in Figure S1 of the SI.

| Region | Photon energy (eV)                  |   |  |
|--------|-------------------------------------|---|--|
|        | [P <sub>66614</sub> ][124Triz] ESD1 | [P <sub>66614</sub> ][124Triz] ESD2 (surface) | [P <sub>66614</sub> ][124Triz] ESD2 (bulk) |
| Survey | 1000                                | 1000  | –  |
| C 1s   | 435                                 | 435   | 885  |
| N 1s   | 550                                 | 550   | 1000                                       |
| O 1s   | 680                                 | 680   | 1130                                       |

**Table 1.** Photon energies used for each XPS region. ESD1 and ESD2 correspond to the two electrospayed thin films of [P<sub>66614</sub>][124Triz], 2.3 and 6.2 nm thick, respectively. Measurements of ESD2 were taken at sampling depths near the surface and in the bulk of the film, achieved by changing the photon energy.

The C 1s region and fitted components are shown in Figure 1 for all stages. The C 1s spectra are intensity normalised to the peak at 285.0 eV. The main C 1s peak at 285 eV can be fitted with two components attributed to the [P<sub>66614</sub>]<sup>+</sup> cation. These occur at 285.0 and 285.7 eV in all stages and are assigned as C<sub>aliphatic</sub> and C<sub>hetero</sub>, respectively (see Scheme 1(a)). These agree with previous reports on the [P<sub>66614</sub>]<sup>+</sup> cation [38]. A third component at 287.1 eV is attributed to carbon atoms in positions 3 and 5 in the [124Triz]<sup>-</sup> anion (C<sup>3,5</sup>).

Exposing the electrospayed IL to CO<sub>2</sub> in Stage 2 results in a gas-phase CO<sub>2</sub> peak at 293.3 eV (not shown) and a carbamate peak (see Scheme 1(b)) at 288.3 eV. As expected, there is no carbamate peak present prior to CO<sub>2</sub> exposure in Stage 1. In addition to a chemical shift of -0.2 eV to 286.9 eV, the C<sup>3,5</sup> component increases in intensity during exposure to CO<sub>2</sub>, reverting to its original intensity and BE when the gas is removed in Stage 3. Similarly, the carbamate peak reduces in intensity but does not reduce to zero when CO<sub>2</sub> is removed, indicating that the reaction with CO<sub>2</sub> is not fully reversible. Hereinafter, this will be referred to as residual carbamate. It has been shown that bulk depositions of [124Triz]<sup>-</sup> ILs reversibly absorb CO<sub>2</sub> by heating the IL, even in the presence of water [26]. A thick film of a similar SBIL has been shown to reversibly absorb and desorb CO<sub>2</sub> by pumping out the gas [31]. However, as shown here, thin films of [P<sub>66614</sub>][124Triz] cannot be regenerated through removing the surrounding gas. Only one CO<sub>2</sub> exposure/desorption stage was recorded in our experiment so we do not know how multiple cycles would affect the uptake and reversibility of absorption. However, in previous work, multiple CO<sub>2</sub> exposure/desorption cycles in the similar SBIL [P<sub>66614</sub>][benzim] were studied using *in situ* attenuated total reflectance-infrared (ATR-IR) spectroscopy as shown in Figures S2 and S3 in the SI. Results show an increase in the carbamate band over multiple exposure/desorption cycles and the presence of small amounts of residual carbamate after desorption, corroborating our XPS data.

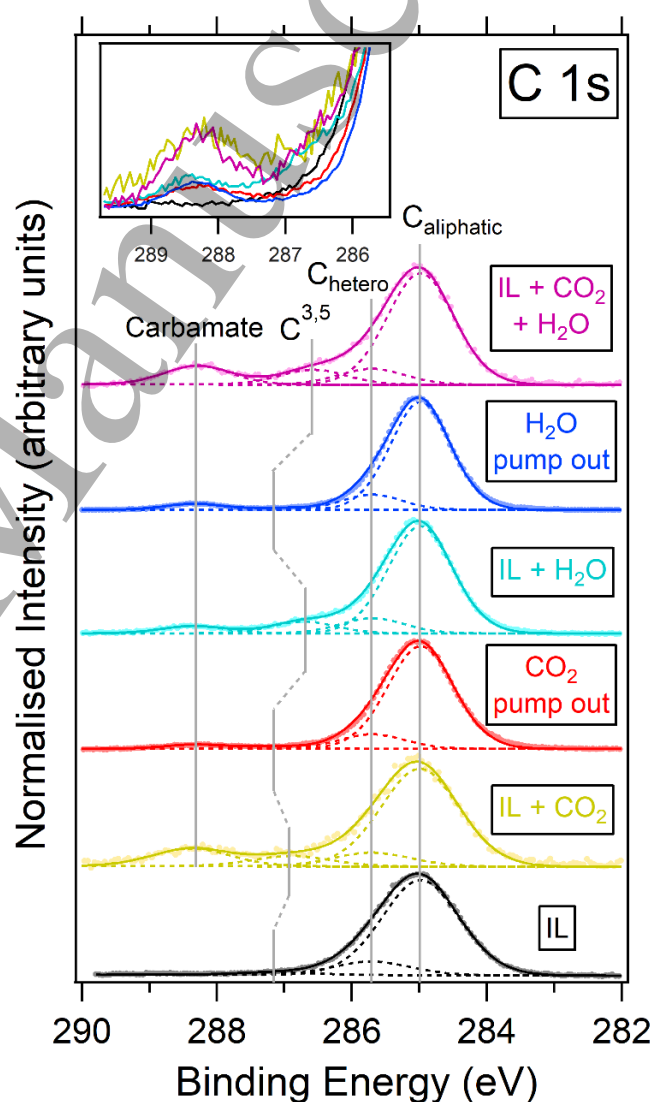


**Figure 1.** C 1s region recorded at a photon energy of 435 eV for an electrospayed thin film of [P<sub>66614</sub>][124Triz] with various exposure regimes of CO<sub>2</sub> and H<sub>2</sub>O at 1 mbar. The highlighted lines show common fitted components. The C<sup>3,5</sup> component shifts downwards in binding energy throughout

the gas exposure stages. The inset shows how the carbamate and  $C^{3.5}$  peaks vary in intensity throughout these stages.

When the IL is exposed to  $H_2O$  in Stage 4 there is no significant change in intensity of the residual carbamate peak. This would suggest that the absorption of  $H_2O$ , which reacts at the same  $N^1$  site as  $CO_2$ , does not remove the irreversibly absorbed  $CO_2$ . The  $C^{3.5}$  component also shifts down to 286.7 eV and increases in intensity, similar behaviour to that found in Stage 2 (IL +  $CO_2$ ). When the  $H_2O$  is removed in Stage 5, the residual carbamate peak persists, suggesting that the absorption and desorption of  $H_2O$  has little effect on the absorbed residual carbamate. Overall, the  $H_2O$  pump out spectrum closely resembles that of the  $CO_2$  pump out stage, with the  $C^{3.5}$  components showing similar intensities and BEs (287.1 eV). This suggests that the IL's reaction with  $H_2O$  is reversible.

When the electrospayed IL is exposed to the  $CO_2/H_2O$  mixture in Stage 6, the carbamate peak increases again to a similar intensity to that of Stage 2 (IL +  $CO_2$ ). This further suggests that the presence of  $H_2O$  does not inhibit the absorption of  $CO_2$  and formation of carbamate, which is in agreement with other reports for  $[124Triz]^-$ -based ILs [26]. Note that the 1 mbar  $CO_2/H_2O$  mixture has an approximately equal number of  $CO_2$  and  $H_2O$  molecules, therefore one might expect the intensity of the carbamate peak to be lower than the 1 mbar  $CO_2$  exposure. The fact that these intensities are similar suggests that a much greater pressure is needed to fully saturate the IL with  $CO_2$ . The  $C^{3.5}$  component (which shifts again to 286.6 eV) also increases to a similar intensity as that in Stages 2 and 4, when the IL is exposed to  $CO_2$  and  $H_2O$ , respectively. The change in BE and intensity of the  $C^{3.5}$  component during gas exposure Stages 2, 4 and 6 is not fully understood. The small BE shifts may be due a change in chemical environment of  $C^{3.5}$  upon chemical reaction or physical interaction between the anion and gas. The change in intensity could be explained by a reordering of anions upon exposure to gas. Note that for the  $CO_2/H_2O$  mixture, reaction between the two gases may form carbonic acid ( $H_2CO_3$ ) [39]. It is possible this may interact with the IL thin film, though we find no evidence of carbonic acid ( $\sim 289$  eV) in our spectra. Note that in this experiment we expose the IL to  $CO_2$  first then  $H_2O$ . If we were to expose the IL to  $H_2O$  first then  $CO_2$ , the reversibility of the reactions may be affected. This would make an interesting further study.

Figure 2 shows the N 1s region for all six stages. The spectra have been normalised by peak area between 396 and 404 eV. The N 1s peak can be fitted with three components, the first two of which at 399.1 and 400.1 eV are assigned to nitrogen species inherent to the  $[124Triz]^-$  anion. The component at 399.1 eV is attributed to  $N^4$  (C–N–C) while the component at 400.1 eV is assigned to the chemically equivalent  $N^1$  and  $N^2$  atoms ( $N^{1,2}$ ).  $N^1$  and  $N^2$  are chemically equivalent due to resonance effects [40], confirmed by

molecular orbital calculations using the software ORCA [41,42]. The IL film was prepared by electrospray in vacuum so we would not expect any significant higher BE peaks attributed to reaction with gas. However, there is a small peak at 401.1 eV which may be due to reactions with trace amounts of gas remaining in the UHV chamber. This peak is assigned to atom  $N^{2,r}$  in the reacted anion. We would expect another peak at higher BE attributed to  $N^{1,r}$  (atom at which gas reacts), but this cannot be resolved here. It is unclear whether the IL has absorbed  $CO_2$ ,  $H_2O$ , or both in this case because the  $N^{2,r}$  component remains at this same BE throughout each of the following exposure stages (the same is also true for the  $N^4$  and  $N^{1,2}$  components).

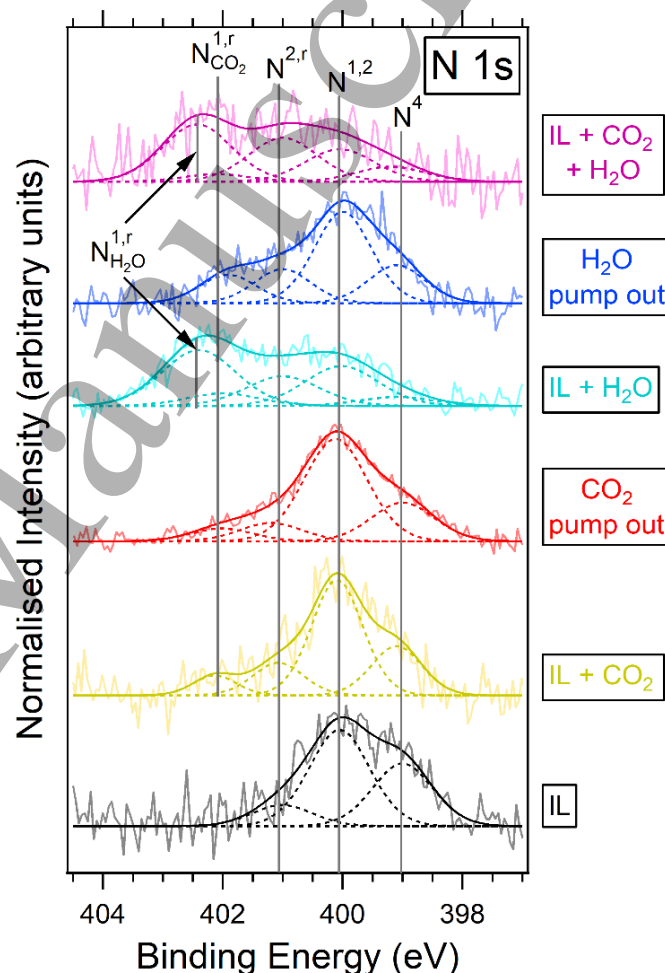


**Figure 2.** N 1s region recorded at a photon energy of 550 eV for an electrospayed thin film of  $[P_{66614}][124Triz]$  with various exposure regimes of  $CO_2$  and  $H_2O$  at 1 mbar. The grey lines show common components fitted through various stages of exposure.

Upon exposure to  $CO_2$  in Stage 2, a peak appears at 402.0 eV. We can assign this to  $N^{1,r}$ , the atom at which carbamate forms ( $N_{CO_2}^{1,r}$ ). Similar to the C 1s region in Figure 1, this carbamate peak reduces in intensity, but not to zero, when the  $CO_2$  is removed in Stage 3, indicating irreversible  $CO_2$

absorption. This residual carbamate peak appears in all following stages, consistent with the C 1s spectra in Figure 1. During these stages all other components remain at similar BEs and intensities as those in Stage 1. The C<sup>3,5</sup> component in the C 1s spectra was found to shift upon exposure to CO<sub>2</sub> (and all subsequent exposure stages), however, we do not see any corresponding chemical shifts in the N 1s region. This is likely due to the level of noise in the data.

When the IL is exposed to H<sub>2</sub>O in Stage 4, a strong peak occurs at 402.4 eV attributed to protonated N<sup>1,r</sup> in H<sub>2</sub>O-reacted [124Triz]<sup>-</sup> (N<sup>1,r</sup><sub>H<sub>2</sub>O</sub>). In previous work in which [P<sub>66614</sub>][benzim] was exposed to a CO<sub>2</sub>/H<sub>2</sub>O mixture, N<sup>1,r</sup><sub>CO<sub>2</sub></sub> and N<sup>1,r</sup><sub>H<sub>2</sub>O</sub> occurred at the same or very similar BEs and could not be individually resolved, resulting in a single reaction component [31]. In the case for [P<sub>66614</sub>][124Triz] in Figure 2, N<sup>1,r</sup><sub>CO<sub>2</sub></sub> and N<sup>1,r</sup><sub>H<sub>2</sub>O</sub> occur at different BEs (402.0 and 402.4 eV, respectively). This is most likely due to the different chemical environments of nitrogen atoms in the [124Triz]<sup>-</sup> anion compared to [benzim]<sup>-</sup>. When H<sub>2</sub>O is removed in Stage 5, the N<sup>1,r</sup><sub>H<sub>2</sub>O</sub> peak at 402.4 eV disappears completely, further indicating that this peak is due to a reversible reaction with H<sub>2</sub>O. This supports previous evidence of reversible H<sub>2</sub>O absorption discussed above (Figure 1). The N<sup>1,r</sup><sub>CO<sub>2</sub></sub> peak appears to be more intense after the H<sub>2</sub>O pump out stage compared to the CO<sub>2</sub> pump out stage. This could indicate a reordering of residual carbamate species to the surface (since measurements were taken at a surface-sensitive photon energy). This is discussed in greater detail below (Figure 4).

Finally, when the IL is exposed to the CO<sub>2</sub>/H<sub>2</sub>O mixture in Stage 6 the spectrum closely resembles that of Stage 4 (IL + H<sub>2</sub>O) except for a more intense N<sup>2,r</sup> component at 401.1 eV. The pressure in Stage 6 rose slightly higher than 1 mbar (1.3 mbar), therefore resulting in a stronger N<sup>2,r</sup> component due to a higher relative concentration of reacted anions. Despite an approximately equal CO<sub>2</sub>:H<sub>2</sub>O molecular ratio in the mixture, the N<sup>1,r</sup><sub>H<sub>2</sub>O</sub> component at 402.4 eV is much more intense than the N<sup>1,r</sup><sub>CO<sub>2</sub></sub> component at 402.0 eV. The reason why H<sub>2</sub>O absorption appears to dominate over CO<sub>2</sub> absorption in Stage 6 will be explored in detail below (see discussion for Figure 4).

Using the N 1s data in Figure 2, the molar uptake ratio of the gases ( $n_{gas}:n_{IL}$ ) was calculated to be 0.3:1 for CO<sub>2</sub>, 0.7:1 for H<sub>2</sub>O, and 0.9:1 for the CO<sub>2</sub>/H<sub>2</sub>O mixture (each with an uncertainty of ± 0.1). For the CO<sub>2</sub>/H<sub>2</sub>O gas mixture, the total molar uptake of 0.9 consists of approximately 0.15 for CO<sub>2</sub> and 0.75 for H<sub>2</sub>O, further suggesting that H<sub>2</sub>O absorption dominates but does not inhibit CO<sub>2</sub> absorption. See the SI for full details of calculations. Looking at the N 1s spectra, we expect less than 1:1 uptake of gas because the unreacted N<sup>1,2</sup> peak is still present in all spectra. If every anion had reacted then the N<sup>1,2</sup> peak would not be visible. The uptake of CO<sub>2</sub> is lower in our experiment than that found by Taylor *et al.* for

the same IL at atmospheric pressure (0.54:1) [30]. This is to be expected as we are exposing a much thinner film of IL to lower pressures of CO<sub>2</sub>.

Another explanation as to why H<sub>2</sub>O absorption dominates over CO<sub>2</sub> absorption in Figure 2 may be that the timescale over which measurements were taken plays an important role. It has been shown that for the IL [BMIM][OAc] the uptake of water into the bulk takes many hours, yet is much quicker at the IL-gas interfacial layers [43]. Conversely, it has been found by Wang *et al.* that bulk thicknesses of phosphonium-based SBILs with similar anions absorbed CO<sub>2</sub> very quickly, on the order of minutes [44,45]. Admittedly these timescales are likely to change at the mbar pressures used in our study compared to atmospheric pressures used by Wang *et al.* Our measurements were taken over a 30 minute timeframe at a surface sensitive sampling depth. Therefore, if [P<sub>66614</sub>][124Triz] is similarly behaved to these ILs, then the reason that H<sub>2</sub>O absorption dominates over CO<sub>2</sub> absorption may be that there is an abundance of H<sub>2</sub>O at the surface due to a slower uptake of the gas into the bulk layers of the IL compared to CO<sub>2</sub>.

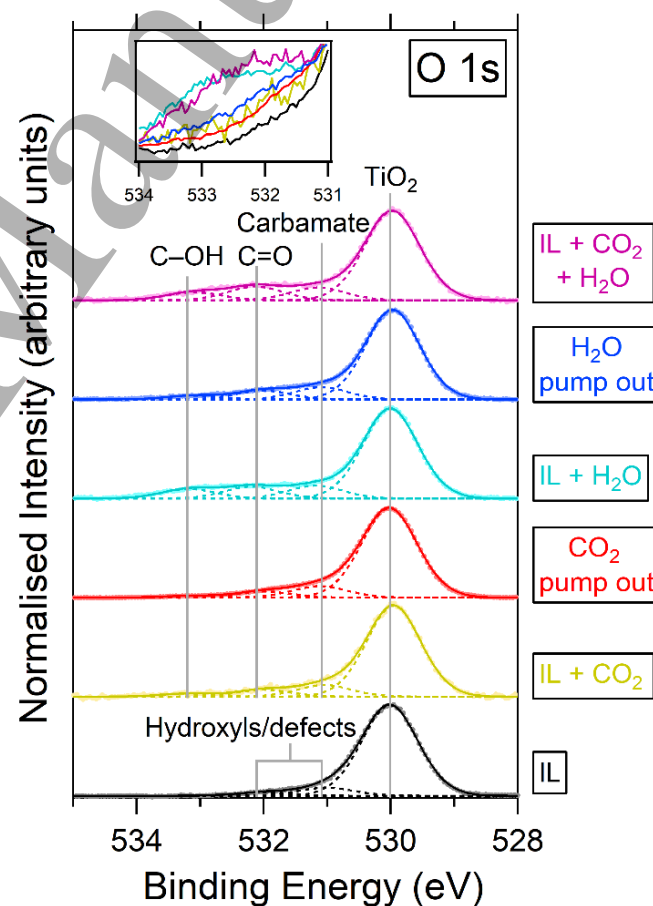


**Figure 3.** O 1s region recorded at a photon energy of 680 eV for an electrospayed thin film of [P<sub>6614</sub>][124Triz] with various exposure regimes of CO<sub>2</sub> and H<sub>2</sub>O at 1 mbar. The grey lines show common components fitted through various stages



of exposure. The inset shows how the broad reaction peak at ~533 eV varies in intensity throughout these stages.

In the O 1s region in Figure 3 there is a common peak at 530.0 eV for all stages, attributed to O atoms in the TiO<sub>2</sub> substrate lattice [46]. The electro sprayed IL (black line) can be fitted with two more components at 531.1 and 532.1 eV. Since there are no oxygen atoms in the IL and we do not see any carbamate species in the C 1s region in Stage 1, we assign these to hydroxyls/defects at the TiO<sub>2</sub> surface [47].

When the electro sprayed IL is exposed to CO<sub>2</sub> (gold line) peaks are fitted at 530.1, 531.1, 532.1, 533.2, and 535.6 eV. These are assigned to TiO<sub>2</sub>, carbamate, C=O in protonated carbamate, C–OH in protonated carbamate, and gas-phase CO<sub>2</sub> (not shown), respectively. Carbamate species formed upon reaction with CO<sub>2</sub> can be protonated and it is likely that there is a mixture of protonated and unprotonated carbamate species present here [48]. The 531.1 and 532.1 eV peaks in Stages 2 – 6 will also contain contributions from the hydroxyl

species/defects at the TiO<sub>2</sub> surface. All fitted components in the O 1s region are summarised in Table 2. When the CO<sub>2</sub> gas is removed in Stage 3 the broad reaction shoulder does not return to the original intensity from Stage 1. This provides further evidence of irreversible CO<sub>2</sub> absorption and reordering in the IL, shown previously in the C 1s and N 1s regions in Figures 1 and 2, respectively.

When the IL is exposed to H<sub>2</sub>O in Stage 4, we see a significant increase in intensity of the reaction components. This would support our assumption that components at 532.1 and 533.2 eV are attributed to interactions with water vapour (C=O and C–OH in protonated carbamate species, respectively). Upon exposure to the CO<sub>2</sub>/H<sub>2</sub>O mixture in the final stage, the broad reaction peak has a similar intensity to that when exposed to H<sub>2</sub>O alone. This suggests that the presence of CO<sub>2</sub> does not inhibit the ad/absorption of H<sub>2</sub>O. The reason why H<sub>2</sub>O absorption appears to dominate over CO<sub>2</sub> absorption in Figure 3 can be explained by exploring absorption at different depths.

| Region | Binding Energy (eV) ± 0.1 eV               | Assignment                                 |
|--------|--|--|
| C 1s   | 285.0                                      | C <sub>aliphatic</sub>                     |
|        | 285.7                                      | C <sub>hetero</sub>                        |
|        | 287.1 <sup>a</sup> → 286.9 → 286.7 → 286.6 | C <sup>3,5</sup>                           |
|        | 288.3                                      | Carbamate                                  |
|        | 293.3                                      | Gas-phase CO <sub>2</sub>                  |
| N 1s   | 399.1                                      | N <sup>4</sup>                             |
|        | 400.1                                      | N <sup>1,2</sup>                           |
|        | 401.1                                      | N <sup>2,r</sup>                           |
|        | 402.0                                      | N <sup>1,r</sup> <sub>CO<sub>2</sub></sub> |
|        | 402.4                                      | N <sup>1,r</sup> <sub>H<sub>2</sub>O</sub> |
| O 1s   | 530.0                                      | TiO <sub>2</sub> lattice O                 |
|        | 531.1                                      | Carbamate <sup>c</sup>                     |
|        | 532.1                                      | C = O <sup>b,c</sup>                       |
|        | 533.2                                      | C – OH <sup>b</sup>                        |
|        | 535.6                                      | Gas-phase H <sub>2</sub> O                 |
|        | 537.0                                      | Gas-phase CO <sub>2</sub>                  |

**Table 2.** Assignments and corresponding BEs of fitted components in the C 1s, N 1s and O 1s regions for [P<sub>66614</sub>][124Triz] for various gas exposure stages. The arrows (→) denote chemical shifts of the C<sup>3,5</sup> component between the following exposure stages: IL → IL + CO<sub>2</sub> → IL + H<sub>2</sub>O → IL + CO<sub>2</sub> + H<sub>2</sub>O. <sup>a</sup> C<sup>3,5</sup> component returns to this BE during the CO<sub>2</sub> and H<sub>2</sub>O pump out stages. <sup>b</sup> Within the protonated carbamate group. <sup>c</sup> These peaks are assigned to hydroxyl species and defects at the TiO<sub>2</sub> surface in Stage 1.

### 3.2 [P<sub>66614</sub>][124Triz] NAP-XPS Depth Study

NAP-XPS was carried out on an electrospayed 6.2 nm thin film of [P<sub>66614</sub>][124Triz] (ESD2) by probing two sampling depths: 4.0 nm to probe the bulk layers of the IL, and 1.6 nm to probe the surface layers. Photoemission measurements were taken for the electrospayed IL, the IL exposed to 1 mbar CO<sub>2</sub>, and the IL exposed to 1 mbar H<sub>2</sub>O, for both bulk and surface sampling depths. Note that these sampling depths are expected to alter slightly during gas exposure stages due to attenuation of electrons through the gas. Since the ESD2 film is formed by depositing more IL on top of the previously measured ESD1 film, we expect some subtle differences in the spectra of the two films. All components remain fitted at approximately the same BEs as those in the previous section.

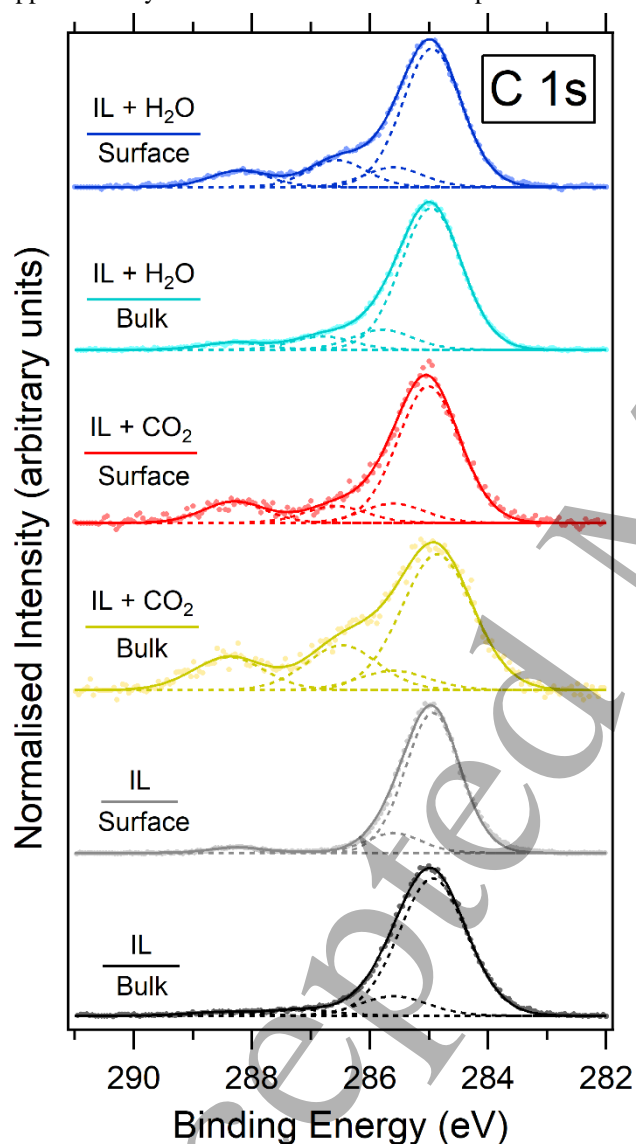


**Figure 4.** XPS of the C 1s region for an electrospayed [P<sub>66614</sub>][124Triz] thin film before exposure, during exposure to CO<sub>2</sub>, and during exposure to H<sub>2</sub>O. The 6.2 nm thick sample was probed at two sampling depths: 4.0 nm to sample the bulk

layers (denoted “Bulk”) and 1.6 nm to sample the surface layers (denoted “Surface”). Surface and bulk sampling depths were recorded at photon energies of 435 and 885 eV, respectively.

Figure 4 shows measurements in the C 1s region, with spectra normalised to the peak at 285.0 eV. For the electrospayed IL, even before exposure to CO<sub>2</sub> there is a small carbamate feature at 288.3 eV for the surface sampling depth (grey line) which may be due to trace amounts of residual CO<sub>2</sub> in the chamber. Alternatively, it could indicate irreversibly absorbed CO<sub>2</sub> from previous exposures (since the ESD2 film was deposited over ESD1), which would further suggest that irreversibly absorbed CO<sub>2</sub> moves to the surface. There has been evidence of irreversible CO<sub>2</sub> absorption in multilayer thin films of the similar IL [P<sub>66614</sub>][benzim] in a previous study [48].

When the IL is exposed to CO<sub>2</sub>, the resulting carbamate peak is more intense for the bulk sampling depth (gold line) compared to the surface (red line). This implies that a greater concentration of carbamate species occurs in the bulk compared to the surface. Lewis *et al.* have reported similar behaviour for aqueous MEA solutions treated with CO<sub>2</sub> [49]. Greater concentrations of CO<sub>2</sub>-reacted MEA were found in the bulk of the solution while unreacted MEA was more concentrated at the surface.

When CO<sub>2</sub> is removed and the IL is exposed to H<sub>2</sub>O alone, a smaller residual carbamate peak remains in the IL + H<sub>2</sub>O spectra (blue lines) at 288.3 eV in Figure 4. Similar evidence of irreversible CO<sub>2</sub> absorption was seen earlier in Figure 1. The residual carbamate peak here is stronger when probed at the surface sampling depth (dark blue line) rather than in the bulk (light blue line), suggesting that more residual carbamate resides at the IL surface than in its bulk layers. In fact, the residual carbamate peak at the surface (dark blue line) is a similar intensity to the carbamate peak at the surface when exposed to CO<sub>2</sub> (red line). This implies that most of the CO<sub>2</sub> that absorbs within the surface layers of the IL does so irreversibly, remaining absorbed when the surrounding gas is pumped out. However, carbamate formed in the bulk (gold line) dramatically reduces in concentration when CO<sub>2</sub> is removed and H<sub>2</sub>O introduced (light blue line). This suggests that the irreversible nature of CO<sub>2</sub> absorption in this IL is largely attributed to reactions at the surface.

To summarise, more CO<sub>2</sub> absorption appears to occur in the bulk of the IL, and this absorption is largely reversible. Less CO<sub>2</sub> adsorbs at the surface and this is irreversible. These results show that both the concentration of carbamate and the level of reversibility varies with depth into the sample.

XPS measurements taken in the N 1s region are shown in Figure 5. The spectra have been normalised by peak area between 396 and 404 eV. For the electrospayed IL, the N 1s peaks are similar at the two sampling depths. As discussed in

Figure 2,  $N^{1,2}$  atoms in the unreacted anion are largely responsible for the main peak centred on 400 eV, implying that the concentration of unreacted anions does not vary significantly through the IL layers prior to exposure.

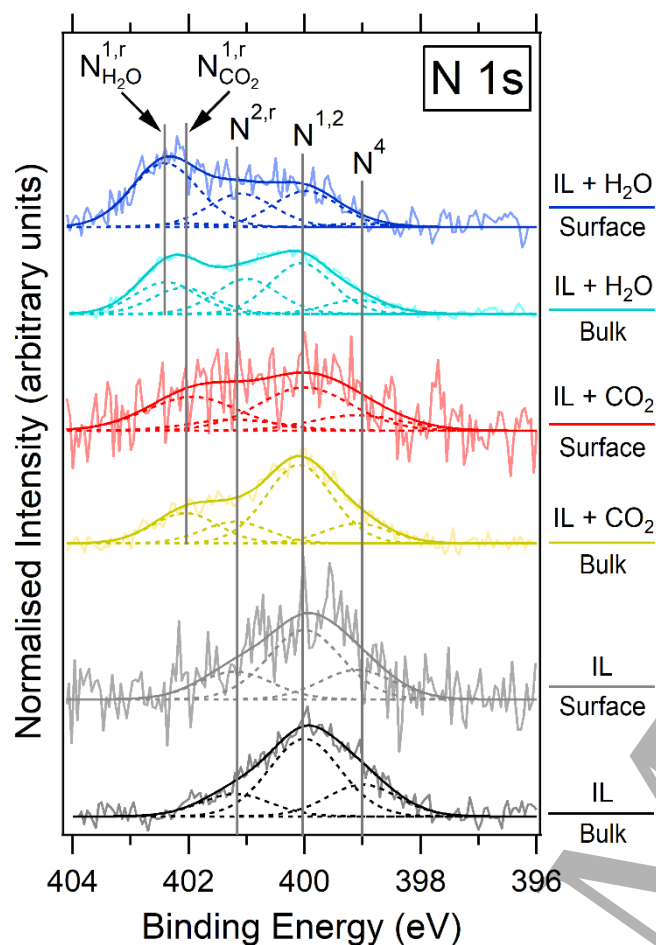


**Figure 5.** XPS of the N 1s region for an electrospayed  $[P_{66614}][124Triz]$  thin film before exposure, during exposure to  $CO_2$ , and during exposure to  $H_2O$ . The 6.2 nm thick sample was probed at two sampling depths: 4.0 nm to sample the bulk layers (denoted “Bulk”) and 1.6 nm to sample the surface layers (denoted “Surface”). Surface and bulk sampling depths were recorded at photon energies of 550 and 1000 eV, respectively.

Upon absorption of  $CO_2$ , a carbamate  $N_{CO_2}^{1,r}$  peak appears at 402.0 eV for both sampling depths. The  $N_{CO_2}^{1,r}$  peak is of higher relative intensity for the surface sampling depth (red line) compared to the bulk (gold line). However, comparing the two is tenuous given the very noisy nature of the surface sampling depth spectrum. This is most likely due to attenuation of photoelectrons through the  $CO_2$  gas, considering they have low kinetic energies (maximum of 150 eV).

The absorption of  $H_2O$  results in protonation of  $N^1$  in  $[124Triz]^-$ , denoted  $N_{H_2O}^{1,r}$ , manifesting as a feature at 402.4 eV. Relative to the main  $N^{1,2}$  peak and the irreversibly

absorbed  $CO_2$   $N_{CO_2}^{1,r}$  peak, the intensity of  $N_{H_2O}^{1,r}$  is greater when probed at the surface (dark blue line) than in the bulk (light blue line). This suggests that there is a greater concentration of protonated N atoms at the surface than in the bulk. This is also supported by the more intense  $C^{3,5}$  (C atoms in the reacted anion) component at the surface when exposed to  $H_2O$  in Figure 4. Results from Figures 4 and 5 suggest that more  $H_2O$ -reacted species remain at the surface of the IL film, and more  $CO_2$ -reacted species diffuse through the surface to the bulk. This would explain why there is little evidence of  $CO_2$  absorption in Figure 3 (O 1s) and why  $H_2O$  absorption appeared to dominate over  $CO_2$  absorption when the IL was exposed to a  $CO_2/H_2O$  mixture in Figure 2 (N 1s), because these spectra were taken at surface-sensitive photon energies of 680 eV and 550 eV, respectively.

In a previous study of the similar IL  $[P_{66614}][benzim]$ , it was found that the presence of  $H_2O$  did not significantly inhibit  $CO_2$  absorption in thin films of the IL at near-ambient pressures [31]. This behaviour could be explained by the results presented here. Reactions between the IL and the two different gases may occur primarily at different depths in the IL film. Additionally, the timescale over which the gases absorb in the IL may play an important role here, as these timescales have been shown to vary significantly for  $CO_2$  and  $H_2O$  in ILs [43,44] (although, these studies used different ILs and atmospheric pressures as opposed to mbar used in our study).

## Discussion

Ordering of IL thin and thick films on solid surfaces has been investigated using a range of other experimental surface-sensitive techniques including angle-resolved NEXAFS [50,51], sum frequency generation (SFG) [52,53], neutron scattering [54,55], atomic force microscopy (AFM) [56], and X-ray reflectivity [57]. Our approach of using XPS at two sampling depths has proven to be another useful tool in analysing the interfacial behaviour of IL thin films on solid surfaces, as well as their interaction with gases. The study presented here is largely qualitative due to limitations of the technique, for example, the high levels of noise as a result of attenuation of photoelectrons through the gas combined with low counts from the use of thin films.

In our thin films, the IL/vacuum and IL/ $TiO_2$  interfaces are likely to have a greater influence than they do in bulk ILs. The ordered structure of ILs at these interfaces is likely to influence specific interactions with  $CO_2/H_2O$  and affect how these gases diffuse from the vacuum interface into the bulk.  $N^1$  and  $N^2$  are equivalent in isolated anions, and we would still expect  $N^1$  and  $N^2$  to remain equivalent at the IL/vacuum interface, however, we expect different ordering at the interface compared to the bulk. The charged parts of the ions in imidazolium-based ILs have been found to form an underlayer near the IL/vacuum interface, with the alkyl chains

of the cations pointing out towards the vacuum [58]. SBILs, such as those used in our experiment, have not been studied as widely in this context. In a previous XPS study of the related SBIL [P<sub>66614</sub>][benzim], C 1s spectra showed a relatively more intense peak associated with the [benzim]<sup>-</sup> anion at grazing emission compared to normal emission, suggesting a higher concentration of [benzim]<sup>-</sup> anions at the IL/vacuum interface compared to the alkyl chains in the [P<sub>66614</sub>]<sup>+</sup> cation [59]. This study provides evidence of SBILs forming an ordered structure at the IL/vacuum interface.

Fundamental studies of ILs at TiO<sub>2</sub> surfaces are sparse so there is very little literature for comparison [16]. Wagstaffe *et al.* studied 4 Å and 30 Å thick films of an imidazolium-based IL at the anatase TiO<sub>2</sub> (101) surface using XPS [51]. They found that in both films the two nitrogen atoms in the imidazolium ring are chemically equivalent and were assigned to a single peak in the N 1s spectra. However, this shifted by 0.2 eV to a lower binding energy in the thinner film due to the interaction of the imidazolium cation with the TiO<sub>2</sub> surface. It is possible that the N<sup>1</sup> and N<sup>2</sup> nitrogen atoms in [124Triz]<sup>-</sup> may react differently with the TiO<sub>2</sub> surface, and this may in turn affect how these anions react with CO<sub>2</sub> or H<sub>2</sub>O. If the anions were to react with the TiO<sub>2</sub> surface this could make them unavailable for reaction with CO<sub>2</sub>/H<sub>2</sub>O. A comprehensive computational study would be required to gain insights into these complex interfacial interactions.

In this study we used electrospray deposition (ESD) to obtain thin films of [P<sub>66614</sub>][124Triz]. It is likely the film is not completely homogeneous and it is possible the IL could form islands on the surface rather than forming layers. However, we are unable to verify the growth mode from our data. Other methods have been used to deposit thin films of ILs, namely physical vapour deposition (PVD) [34,51,60] and dip-coating [56,61]. Each have their own advantages and disadvantages; for example, PVD requires thermally stable ILs while ESD does not. ESD allows thin films of large molecules to be deposited *in situ* in ultra-high vacuum [62]. However, electrosprayed thin films can have an unequal concentration of cations and anions compared to PVD due to the increased diffusion of cations and anions with positive and negative tip biases, respectively [63]. ESD of ILs is comparatively underutilised, and prior to this study has not been used to deposit large IL molecules or used alongside NAP-XPS to investigate gas capture in thin films of ILs, to the best of our knowledge.

The results presented here have implications for thin film IL-based technologies. For example, thin films of ILs have been used to modify conventional supported catalysts, allowing the selectivity of the solid catalyst to be fine-tuned and improved (SCILL and SILP catalysis) [64]. A problem these technologies face is their sensitivity to changes at the IL/gas phase and IL/solid support interfaces [65]. Therefore, adsorption of gaseous/liquid reactants, products or

contaminants in SCILL/SILP catalysts may induce changes in the surface structure of the IL thin film, potentially impacting the diffusion and selectivity for intermediate products in these catalysts [15].

## Conclusion

The competitive absorption between CO<sub>2</sub> and H<sub>2</sub>O in electrosprayed thin films of the superbasic IL [P<sub>66614</sub>][124Triz] has been characterised using *in situ* NAP-XPS. To the best of our knowledge, [P<sub>66614</sub>]<sup>+</sup> is the largest IL ion to be successfully deposited via electrospray. Results suggest that both reacted and unreacted [124Triz]<sup>-</sup> anions reorder and diffuse through the IL thin film upon exposure to CO<sub>2</sub> and/or H<sub>2</sub>O. The NAP-XPS depth study revealed that greater concentrations of CO<sub>2</sub>-reacted species appear in the bulk layers of an electrosprayed IL thin film, reversibly forming carbamate on the anion. However, fewer CO<sub>2</sub>-reacted species appear at the surface layers, and this reaction is irreversible. H<sub>2</sub>O vapour adsorbs in greater concentrations at the surface rather than the bulk but does not inhibit the absorption of CO<sub>2</sub>. The molar uptake ratio of gases ( $n_{gas} \cdot n_{IL}$ ) in the electrosprayed IL was calculated to be 0.3:1 for CO<sub>2</sub>, 0.7:1 for H<sub>2</sub>O, and 0.9:1 for the CO<sub>2</sub>/H<sub>2</sub>O mixture (each with an uncertainty of  $\pm 0.1$ ). To the best of our knowledge, this is the first use of a NAP-XPS at different depths to study gas absorption in ILs. Reordering of IL thin films upon contamination with air and water vapour may also affect the performance of IL thin film-based technologies such as SCILL/SILP catalysis, IL lubricants and corrosion inhibitors.

## Acknowledgements

We acknowledge MAX IV Laboratory for time on HIPPIE Beamline under Proposal 20180137. Research conducted at MAX IV, a Swedish national user facility, is supported by the Swedish Research council under contract 2018-07152, the Swedish Governmental Agency for Innovation Systems under contract 2018-04969, and Formas under contract 2019-02496. The research leading to this result has been supported by the project CALIPSOplus under the Grant Agreement 730872 from the EU Framework Programme for Research and Innovation HORIZON 2020. AT acknowledges funding via the Henry Royce Institute for Advanced Materials, funded through EPSRC grants EP/R00661X/1 and EP/P025021/1. The authors acknowledge the Jeremiah Horrocks Institute for the PhD studentships for ZH and JC.

## References

- [1] Rao A B and Rubin E S 2006 Identifying cost-effective CO<sub>2</sub> control levels for amine-based CO<sub>2</sub> capture systems *Ind. Eng. Chem. Res.* **45** 2421–9
- [2] Cuéllar-Franca R M and Azapagic A 2015 Carbon capture, storage and utilisation technologies: A

- critical analysis and comparison of their life cycle environmental impacts *J. CO<sub>2</sub> Util.* **9** 82–102
- [3] Welton T 2018 Ionic liquids: a brief history *Biophys. Rev.* **10** 691–706
- [4] Yu C H, Huang C H and Tan C S 2012 A review of CO<sub>2</sub> capture by absorption and adsorption *Aerosol Air Qual. Res.* **12** 745–69
- [5] Cuéllar-Franca R M, García-Gutiérrez P, Taylor S F R, Hardacre C and Azapagic A 2016 A novel methodology for assessing the environmental sustainability of ionic liquids used for CO<sub>2</sub> capture *Faraday Discuss.* **192** 283–301
- [6] Bates E D, Mayton R D, Ntai I and Davis J H 2002 CO<sub>2</sub> capture by a task-specific ionic liquid *J. Am. Chem. Soc.* **124** 926–7
- [7] Macfarlane D R, Tachikawa N, Forsyth M, Pringle J M, Howlett P C, Elliott G D, Davis J H, Watanabe M, Simon P and Angell C A 2014 Energy applications of ionic liquids *Energy Environ. Sci.* **7** 232–50
- [8] Li H, Qu J, Cui Q, Xu H, Luo H, Chi M, Meisner R A, Wang W and Dai S 2011 TiO<sub>2</sub> nanotube arrays grown in ionic liquids: high-efficiency in photocatalysis and pore-widening *J. Mater. Chem.* **21** 9487
- [9] Li X, Zhao Z and Pan C 2016 Ionic liquid-assisted electrochemical exfoliation of carbon dots of different size for fluorescent imaging of bacteria by tuning the water fraction in electrolyte *Microchim. Acta* **183** 2525–32
- [10] Roy P, Kim D, Lee K, Spiecker E and Schmuki P 2010 TiO<sub>2</sub> nanotubes and their application in dye-sensitized solar cells *Nanoscale* **2** 45–59
- [11] Bai S, Da P, Li C, Wang Z, Yuan Z, Fu F, Kawecki M, Liu X, Sakai N, Wang J T W, Huettner S, Buecheler S, Fahlman M, Gao F and Snaith H J 2019 Planar perovskite solar cells with long-term stability using ionic liquid additives *Nature* **571** 245–50
- [12] Minami I 2009 Ionic liquids in tribology. *Molecules* **14** 2286–305
- [13] Somers A E, Howlett P C, MacFarlane D R and Forsyth M 2013 A review of ionic liquid lubricants *Lubricants* **1** 3–21
- [14] Zhou F, Liang Y and Liu W 2009 Ionic liquid lubricants: Designed chemistry for engineering applications *Chem. Soc. Rev.* **38** 2590–9
- [15] Steinrück H P and Wasserscheid P 2015 Ionic liquids in catalysis *Catal. Letters* **145** 380–97
- [16] Cole J and Syres K L 2022 Ionic liquids on oxide surfaces *J. Phys. Condens. Matter* **34** 213002
- [17] Porter R T J, Fairweather M, Pourkashanian M and Woolley R M 2015 The range and level of impurities in CO<sub>2</sub> streams from different carbon capture sources *Int. J. Greenh. Gas Control* **36** 161–74
- [18] Xu X, Song C, Wincek R, Andresen J M, Miller B G and Scaroni A W 2003 Separation of CO<sub>2</sub> from Power Plant Flue Gas Using a Novel CO<sub>2</sub> “Molecular Basket” Adsorbent *ACS Div. Fuel Chem. Prepr.* **48** 162–3
- [19] Lei Z, Dai C and Chen B 2014 Gas solubility in ionic liquids *Chem. Rev.* **114** 1289–326
- [20] Boot-Handford M E, Abanades J C, Anthony E J, Blunt M J, Brandani S, Mac Dowell N, Fernández J R, Ferrari M C, Gross R, Hallett J P, Haszeldine R S, Heptonstall P, Lyngfelt A, Makuch Z, Mangano E, Porter R T J, Pourkashanian M, Rochelle G T, Shah N, Yao J G and Fennell P S 2014 Carbon capture and storage update *Energy Environ. Sci.* **7** 130–89
- [21] Grishina E P, Ramenskaya L M, Gruzdev M S and Kraeva O V. 2013 Water effect on physicochemical properties of 1-butyl-3-methylimidazolium based ionic liquids with inorganic anions *J. Mol. Liq.* **177** 267–72
- [22] Zhang X, Zhang X, Dong H, Zhao Z, Zhang S and Huang Y 2012 Carbon capture with ionic liquids: Overview and progress *Energy Environ. Sci.* **5** 6668–81
- [23] Liang Z (Henry), Rongwong W, Liu H, Fu K, Gao H, Cao F, Zhang R, Sema T, Henni A, Sumon K, Nath D, Gelowitz D, Srisang W, Saiwan C, Benamor A, Al-Marri M, Shi H, Supap T, Chan C, Zhou Q, Abu-Zahra M, Wilson M, Olson W, Idem R and Tontiwachwuthikul P (PT) 2015 Recent progress and new developments in post-combustion carbon-capture technology with amine based solvents *Int. J. Greenh. Gas Control* **40** 26–54
- [24] Babamohammadi S, Shamiri A and Aroua M K 2015 A review of CO<sub>2</sub> capture by absorption in ionic liquid-based solvents *Rev. Chem. Eng.* **31** 383–412
- [25] Greer A J, Taylor S F R, Daly H, Quesne M, Catlow C R A, Jacquemin J and Hardacre C 2019 Investigating the effect of NO on the capture of CO<sub>2</sub> using superbase ionic liquids for flue gas applications *ACS Sustain. Chem. Eng.* **7** 3567–74
- [26] Taylor S F R, McCrellis C, McStay C, Jacquemin J, Hardacre C, Mercy M, Bell R G and De Leeuw N H 2015 CO<sub>2</sub> capture in wet and dry superbase ionic liquids *J. Solution Chem.* **44** 511–27
- [27] McCrellis C, Taylor S F R, Jacquemin J and Hardacre C 2016 Effect of the Presence of MEA on the CO<sub>2</sub> Capture Ability of Superbase Ionic Liquids *J. Chem. Eng. Data* **61** 1092–100
- [28] Hollingsworth N, Taylor S F R, Galante M T, Jacquemin J, Longo C, Holt K B, De Leeuw N H and Hardacre C 2015 CO<sub>2</sub> capture and electrochemical conversion using superbasic [P66614][124Triz] *Faraday Discuss.* **183** 389–400
- [29] Mercy M, Rebecca Taylor S F, Jacquemin J, Hardacre C, Bell R G and De Leeuw N H 2015 The addition of CO<sub>2</sub> to four superbase ionic liquids: a DFT study *Phys. Chem. Chem. Phys.* **17** 28674–82
- [30] Taylor S F R, McClung M, McReynolds C, Daly H, Greer A J, Jacquemin J and Hardacre C 2018 Understanding the Competitive Gas Absorption of CO<sub>2</sub> and SO<sub>2</sub> in Superbase Ionic Liquids *Ind. Eng. Chem. Res.* **57** 17033–42

- [31] Henderson Z, Thomas A G, Wagstaffe M, Taylor S F R, Hardacre C and Syres K L 2019 Reversible reaction of CO<sub>2</sub> with superbasic ionic liquid [P66614][benzim] studied with in situ photoelectron spectroscopy *J. Phys. Chem. C* **123** 7134–41
- [32] Schnadt J, Knudsen J and Johansson N 2020 Present and new frontiers in materials research by ambient pressure x-ray photoelectron spectroscopy *J. Phys. Condens. Matter* **32**
- [33] Khalifa Y, Broderick A and Newberg J T 2018 Surface enhancement of water at the ionic liquid-gas interface of [HMIM][Cl] under ambient water vapor *J. Phys. Condens. Matter* **30** 325001
- [34] Henderson Z, Walton A S, Thomas A G and Syres K L 2018 Water-induced reordering in ultrathin ionic liquid films *J. Phys. Condens. Matter* **30** 334003
- [35] Niedermaier I, Bahlmann M, Papp C, Kolbeck C, Wei W, Krick Calderón S, Grabau M, Schulz P S, Wasserscheid P, Steinrück H P and Maier F 2014 Carbon dioxide capture by an amine functionalized ionic liquid: Fundamental differences of surface and bulk behavior *J. Am. Chem. Soc.* **136** 436–41
- [36] Zhu S, Scardamaglia M, Kundsén J, Sankari R, Tarawneh H, Temperton R, Pickworth L, Cavalca F, Wang C, Tissot H, Weissenrieder J, Hagman B, Gustafson J, Kaya S, Lindgren F, Kallquist I, Maibach J, Hahlin M, Boix V, Gallo T, Rehman F, D'Acunto G, Schnadt J and Shavorskiy A 2021 HIPPIE: A new platform for ambient-pressure X-ray photoelectron spectroscopy at the MAX IV Laboratory *J. Synchrotron Radiat.* **28** 624–36
- [37] Fairely N 2009 CasaXPS manual 2.3.15 *Casa Softw. Ltd* 1–177
- [38] Blundell R K and Licence P 2014 Quaternary ammonium and phosphonium based ionic liquids: A comparison of common anions *Phys. Chem. Chem. Phys.* **16** 15278–88
- [39] Hollingsworth N, Taylor S F R, Galante M T, Jacquemin J, Longo C, Holt K B, de Leeuw N H and Hardacre C 2015 Reduction of Carbon Dioxide to Formate at Low Overpotential Using a Superbase Ionic Liquid *Angew. Chemie* **127** 14370–4
- [40] Lovelock K R J, Smith E F, Deyko A, Villar-Garcia I J, Licence P and Jones R G 2007 Water adsorption on a liquid surface *Chem. Commun.* 4866–8
- [41] Neese F 2012 The ORCA program system *Wiley Interdiscip. Rev. Comput. Mol. Sci.* **2** 73–8
- [42] Neese F 2018 Software update: the ORCA program system, version 4.0 *Wiley Interdiscip. Rev. Comput. Mol. Sci.* **8** 4–9
- [43] Broderick A, Khalifa Y, Shiflett M B and Newberg J T 2017 Water at the Ionic Liquid-Gas Interface Examined by Ambient Pressure X-ray Photoelectron Spectroscopy *J. Phys. Chem. C* **121** 7337–43
- [44] Wang C, Luo X, Luo H, Jiang D, Li H and Dai S 2011 Tuning the basicity of ionic liquids for equimolar CO<sub>2</sub> capture *Angew. Chemie* **123** 5020–4
- [45] Zeng S, Zhang X, Bai L, Zhang X, Wang H, Wang J, Bao D, Li M, Liu X and Zhang S 2017 Ionic-Liquid-Based CO<sub>2</sub> Capture Systems: Structure, Interaction and Process *Chem. Rev.* **117** 9625–73
- [46] Syres K L, Thomas A G, Flavell W R, Spencer B F, Bondino F, Malvestuto M, Preobrajenski A and Grätzel M 2012 Adsorbate-induced modification of surface electronic structure: Pyrocatechol adsorption on the anatase TiO<sub>2</sub> (101) and rutile TiO<sub>2</sub> (110) surfaces *J. Phys. Chem. C* **116** 23515–25
- [47] Jackman M J, Thomas A G and Muryn C 2015 Photoelectron spectroscopy study of stoichiometric and reduced anatase TiO<sub>2</sub>(101) surfaces: The effect of subsurface defects on water adsorption at near-ambient pressures *J. Phys. Chem. C* **119** 13682–90
- [48] Cole J, Henderson Z, Thomas A G, Compeán-González C L, Greer A J, Hardacre C, Venturini F, Garzon W Q, Ferrer P, Grinter D C, Held G and Syres K L 2021 Near-Ambient Pressure XPS and NEXAFS Study of a Superbasic Ionic Liquid with CO<sub>2</sub> *J. Phys. Chem. C* **125** 22778–85
- [49] Lewis T, Faubel M, Winter B and Hemminger J C 2011 CO<sub>2</sub> capture in amine-based aqueous solution: Role of the gas-solution interface *Angew. Chemie - Int. Ed.* **50** 10178–81
- [50] Walsh J F, Dhariwal H S, Gutiérrez-Sosa A, Finetti P, Muryn C A, Brookes N B, Oldman R J and Thornton G 1998 Probing molecular orientation in corrosion inhibition via a NEXAFS study of benzotriazole and related molecules on Cu(100) *Surf. Sci.* **415** 423–32
- [51] Wagstaffe M, Jackman M J, Syres K L, Generalov A and Thomas A G 2016 Ionic Liquid Ordering at an Oxide Surface *ChemPhysChem* **17** 3430–4
- [52] Rivera-Rubero S and Baldelli S 2004 Influence of water on the surface of hydrophilic and hydrophobic room-temperature ionic liquids *J. Am. Chem. Soc.* **126** 11788–9
- [53] Baldelli S 2008 Surface structure at the ionic liquid-electrified metal interface *Acc. Chem. Res.* **41** 421–31
- [54] Bowers J, Vergara-Gutierrez M C and Webster J R P 2004 Surface Ordering of Amphiphilic Ionic Liquids *Langmuir* **20** 309–12
- [55] Bovio S, Podestà A, Lenardi C and Milani P 2009 Evidence of extended solidlike layering in [Bmim][NTf<sub>2</sub>] ionic liquid thin films at room-temperature *J. Phys. Chem. B* **113** 6600–3
- [56] Zhao W, Zhu M, Mo Y and Bai M 2009 Effect of anion on micro/nano-tribological properties of ultrathin imidazolium ionic liquid films on silicon wafer *Colloids Surfaces A Physicochem. Eng. Asp.* **332** 78–83
- [57] Solutskin E, Ocko B M, Taman L, Kuzmenko I, Gog T and Deutsch M 2005 Surface layering in ionic liquids: An x-ray reflectivity study *J. Am. Chem. Soc.* **127** 7796–804
- [58] Lockett V, Sedev R, Bassell C and Ralston J 2008 Angle-resolved X-ray photoelectron spectroscopy of

- 1  
2  
3 the surface of imidazolium ionic liquids *Phys. Chem.*  
4 *Chem. Phys.* **10** 1330–5
- 5 [59] Cole J, Henderson Z, Thomas A G, Compeán-  
6 González C L, Greer A J, Hardacre C, Venturini F,  
7 Garzon W Q, Ferrer P, Grinter D C, Held G and  
8 Syres K L 2021 Near-Ambient Pressure XPS and  
9 NEXAFS Study of a Superbasic Ionic Liquid with  
10 CO<sub>2</sub> *J. Phys. Chem. C* **125** 22778–85
- 11 [60] Cremer T, Killian M, Gottfried J M, Paape N,  
12 Wasserscheid P, Maier F and Steinrück H P 2008  
13 Physical vapor deposition of [EMIM][Tf<sub>2</sub>N]: A new  
14 approach to the modification of surface properties  
15 with ultrathin ionic liquid films *ChemPhysChem* **9**  
16 2185–90
- 17 [61] Palacio M and Bhushan B 2008 Ultrathin wear-  
18 resistant ionic liquid films for novel MEMS/NEMS  
19 applications *Adv. Mater.* **20** 1194–8
- 20 [62] Swarbrick J C, Taylor J Ben and O’Shea J N 2006  
21 Electro spray deposition in vacuum *Appl. Surf. Sci.*  
22 **252** 5622–6
- 23 [63] Rietzler F, Piermaier M, Deyko A, Steinrück H P  
24 and Maier F 2014 Electro spray ionization deposition  
25 of ultrathin ionic liquid films: [C<sub>8</sub>C<sub>1</sub>Im]Cl and  
26 [C<sub>8</sub>C<sub>1</sub>Im][Tf<sub>2</sub>N] on Au(111) *Langmuir* **30** 1063–71
- 27 [64] Steinrück H P, Libuda J, Wasserscheid P, Cremer T,  
28 Kolbeck C, Laurin M, Maier F, Sobota M, Schulz P  
29 S and Stark M 2011 Surface science and model  
30 catalysis with ionic liquid-modified materials *Adv.*  
31 *Mater.* **23** 2571–87
- 32 [65] Fehrmann R, Riisager A and Haumann M 2014  
33 *Supported Ionic Liquids: Fundamentals and*  
34 *Applications* ed R Fehrmann, A Riisager and M  
35 Haumann (Weinheim, Germany: Wiley-VCH Verlag  
36 GmbH & Co. KGaA)
- 37  
38  
39  
40  
41  
42  
43  
44  
45  
46  
47  
48  
49  
50  
51  
52  
53  
54  
55  
56  
57  
58  
59  
60